

## Assessment on resilience of urban agglomeration transportation system considering passenger choice and load-capacity factor



Zhicheng Yang<sup>a</sup>, Xiaobing Liu<sup>b,\*</sup>, Jiangfeng Wang<sup>a,\*</sup>, Xuedong Yan<sup>a</sup>, Rui Shen<sup>a</sup>, Zhengqi Huo<sup>b</sup>

<sup>a</sup> School of Traffic and Transportation, Beijing Jiaotong University, No.3 Shangyuancun Haidian District, Beijing 100044, PR China

<sup>b</sup> School of System Science, Beijing Jiaotong University, No.3 Shangyuancun Haidian District, Beijing 100044, PR China

### ARTICLE INFO

#### Key words:

Comprehensive transportation  
Network resilience  
Mobile signaling data  
Path choice  
Cascading failure

### ABSTRACT

Intercity transportation system (ICTS), characterized by large-scale, high spatial-temporal concentration, and sparser departure frequencies, is more vulnerable in unexpected events. Understanding the resilience characteristics of ICTS is crucial for maintaining the network service capabilities. Aiming to conduct effective resilience assessment on ICTS, we develop the resilience simulation model by introduce dual-regulated parameters for network load and capacity into cascading propagation model under interruption events, and quantify the impact of travel distance, time costs, and route redundancy on travel choice of passengers. Meanwhile, propose service resilience indicators from both the passenger's and the system's perspectives. Finally, we conduct a case study on the resilience of ICTS in Beijing-Tianjin-Hebei Urban Agglomerations (BTH-UA). The results show that: 1) Multimodal transportation systems usually exhibit better resilience than unimodal systems. 2) For various resilience optimization metrics, it is essential to choose targeted recovery strategies to maximize network resilience. 3) Traveler sensitivity to travel time significantly influences the resilience of passenger-based network services. 4) Changes in transportation supply capacity and travel demand will impact the system's resilience. The research findings can provide valuable references for the resilience development and management of urban transportation systems.

### 1. Introduction

In the process of urbanization, urban agglomerations, as one of the most important carriers for economic development in the context of globalization, have gradually replaced cities as the basic regional units for global competition and division of labor [1,2]. ICTS as a crucial medium for population, goods, financial, and information flows between cities, plays a significant supporting role in shaping the spatial structure of urban agglomerations and promoting their economic development [3-7].

The ICTS of urban agglomerations is a complex system with the characteristics of multi-scale, multimodal, high randomness, and dynamism. Compared to intra-city travel, intercity travel exhibits longer travel distances, higher spatial-temporal concentration and sparser departure frequencies, which make the function of ICTS more uncertain and vulnerable [8]. Natural disruptions (such as floods, hurricanes, and earthquakes) and human-induced disruptions (such as terrorist attacks and traffic accidents) can cause severe impacts on ICTS once they occur [9]. Therefore, it is necessary to study the performance of ICTS in the

face of disasters, so as to better meet the needs of regional transportation network maintenance and achieve further improvement of network service capabilities.

In fact, assessing and developing more resilient transportation systems in the face of disasters has attracted more and more attention in recent years [10-14]. The concept of resilience in transportation systems refers to the ability of a system to maintain its functionality in the face of destructive events or disturbances [15]. The introduction of resilience provides a tool for understanding the process of system adaptation, absorption, and recovery from various perturbations and failures [10]. Previous studies on transportation network resilience mostly focus on unimodal subsystems, such as aviation networks [16], railway networks [17], urban rail transit networks [18], etc. Currently, more research considered the coupling of different modes of transportation [19-22] or the complementary effects between different modes of transportation [23].

In terms of urban agglomeration transportation, scholars attempted to construct comprehensive transportation networks that incorporate multiple modes of transportation and evaluate their resilience

\* Corresponding authors at: Beijing Jiaotong University, No. 3 Shangyuancun Haidian District, Beijing 100044, PR China.

E-mail address: [lxiaobing@bjtu.edu.cn](mailto:lxiaobing@bjtu.edu.cn) (X. Liu).

performance under various scenarios, including random failures, deliberate attacks, and natural disasters [24,25]. The research results indicate that urban agglomeration transportation networks are more vulnerable under targeted attacks [24]. As one of the typical phenomenon of network transportation resilience, cascade failure refers to that the failure of a single station or line causes partial or even the whole network to collapse due to passenger flow redistribution, which attracts wide attentions of scholars and administrators [26-30]. When facing cascade failure caused by traffic disruptions, there has been a consensus that the performance of networks under different load levels and passenger flow structures varies [25,31,32].

From the perspective of network capacity, The load-capacity model proposed by Motter and Lai is one of the most classical models for cascade failure analysis [33]. The current load-capacity models can be roughly divided into linear and nonlinear categories. Linear load-capacity models set the initial load of the network and introduce a tolerance parameter to calculate the network's maximum capacity. When the load on a node exceeds its maximum capacity, the node fails [34]. This method assumes a positive correlation between node capacity and load, which is in line with people's general understanding, so it is widely used in cascaded failure modeling of complex networks [35-39]. Nonlinear load-capacity models define the initial load and introduce a tolerance parameter describing an exponential relationship to calculate the maximum capacity of nodes [22,40,41]. When analyzing the process of cascade failure, the above two methods change the capacity of network nodes by adjusting tolerance parameter, to analyze the influence of network load-capacity relationship on the scale of network cascade failure. However, recent studies have shown that in transportation networks, in addition to network capacity, the increase of network load will also aggravate the impact of cascade failure [29]. Simply adjusting capacity control parameters cannot reflect situations where both capacity and load change simultaneously, and the resilience characteristics of networks with different levels of network load under varying network capacities have not been explored.

From the perspective of network structure, traditional studies mainly observe the performance of systems in response to disruptions from a network topology perspective [42,43]. With increasing attention to the service characteristics of transportation systems, recent research has gradually shifted towards the functional resilience of transportation networks [44]. Some scholars developed dynamic network resilience frameworks that can respond to disruptions without external intervention, capturing the dynamic changes in network performance during destructive events [45], and some researchers measured key attributes of resilience in stages throughout the process of disturbances [46]. Moreover, Zhong et al. argued the propagation of network failures is caused by the redistribution of network flows [31]. Unexpected events in transportation networks do not change the destination of passengers but only affect the routes they choose to reach their destinations [47]. The interactive between network function and traveler rerouting behavior can serve as an important entry point for measuring system resilience [48]. Although some researchers have recognized the impact of passenger choice behavior on system performance during disruption events [14,29] and designed travel time based functional resilience measurement indicators before and after disruptions [49], there are still some key issues that need to be addressed. First, there is lacking a resilience assessment framework designed from the perspective of individual passengers. Second, the quantification analysis on the influence of passenger choice behavior on the service characteristics and system resilience of transportation network during disruption events were rarely discussed by researchers.

Compared to traditional resilience research methods based on simulation [50,51] and models [52,53], the advent of the big data provides us with great opportunities to timely access comprehensive transportation information and explore the characteristics of passenger behavior and transportation system resilience in large-scale urban agglomerations [8]. In comparison to floating car data and public transport

card data, mobile signaling data, as one of the mobile big data, not only contains personal spatiotemporal trajectory information but also reflects individual mobility patterns and characteristics of group travel distribution [54,55]. It is characterized by large data volume, wide coverage, and high sampling frequency, enabling a better representation of residents' travel information at the urban agglomeration scale. Therefore, mobile signaling data has been widely used to analyze various problems caused by human mobility at the scale of urban agglomerations [56-59], including studies on the mobility pattern of urban agglomerations [56], commuting structure [57], evaluation of urban integration level [58] and urban spatial pattern [59]. However, current research on the resilience of ICTS based on mobile signaling data is relatively lacking.

To fill the above research gaps, we propose a new resilience simulation framework, as shown in Fig. 1, which includes the construction of a transportation network, the development of a cascading failure model, and the design of a simulation module for real-world cases. First, we construct a passenger-centric comprehensive intercity transportation service network within the urban agglomeration based on mobile signaling data, station location data, and train timetables. Second, we establish a cascading failure model that considers passenger path choice and infrastructure capacity constraints. Finally, we study the resilience of the ICTS within the urban agglomeration from both the passenger and infrastructure perspectives. In comparison to previous studies, this paper makes the following main contributions:

1. A cascading failure propagation model that considers both network capacity constraints and travelers' path choice tendencies in the face of disruption events is first proposed to investigate the resilience of ICTS.
2. Considering the influence of travel distance, time cost and route redundancy on passengers, combined with intercity transfer demand, the travel choice of passengers was quantified. A dual-factor capacity-loading model for bus and train is designed to quantify the impact of network supply-demand relationship on system resilience.
3. This paper proposes passenger service indicator and system service indicator from two perspectives: passenger travel service demand and system supply service capacity. The passenger service indicator evaluates the level of satisfaction of passenger travel demands based on the success rate of passenger transfer, while the system service indicator assesses the service capacity of the transport network in terms of maximum transportation capacity per unit time. Subsequently, we establish passenger service resilience indicator and system service resilience indicator based on these two metrics.
4. We analyze the differences in resilience between railway transportation system (RTS) and comprehensive transportation system (CTS), and explore the impact of node recovery strategy, passenger choice behavior, station capacity parameters, and network load parameters on system resilience in case study. The results can provide valuable information for promoting the resilience of urban agglomeration transportation systems.

The rest of this paper is organized as follows. Section 2 presents the process of constructing the transportation network and the cascading failure model. Section 3 provides a research case based on the BTH-UA. Section 4 discusses the simulation results and limitations of the study. Section 5 summarizes the research findings.

## 2. Methodology

### 2.1. Network description

In the ICTS of urban agglomerations, there are multiple transportation modes such as railways, roads, and aviation. Among them, railways and roads play a more significant role in intercity transportation, as they are mutually coupled and jointly bear the main

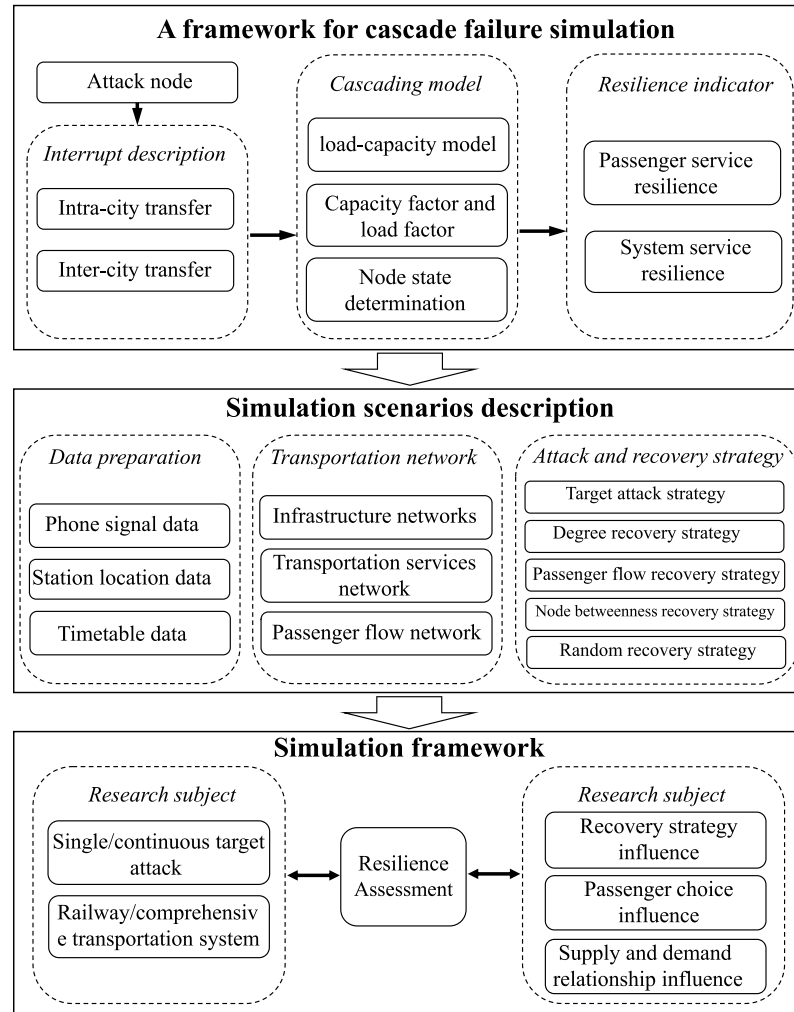


Fig. 1. Research framework.

transportation tasks for passengers [25]. Therefore, in this study, we consider the construction of an intercity comprehensive public transportation system using both railway and road transportation modes.

We describe the intercity public transportation network of urban agglomerations as a multi-level network model composed of infrastructure network, transportation service network, and passenger flow network. The infrastructure network refers to the network of facilities and equipment including railway stations, long-distance bus stations, railway lines, and roadways, which provide support for the provision of transportation services. The transportation service network is an abstract service network formed by the locations of stations and train transport routes, which determines the level of transportation service supply. The passenger flow network refers to the intercity travel network, reflecting the level of intercity travel demand in urban agglomerations. In this paper, we use intercity travel mobile signaling OD data to generate the intercity travel passenger flow network. The following section provides the method for constructing the service network and the process of generating the passenger flow network using intercity mobile signaling OD data.

### 2.1.1. Service network construction

P-Space refers to a modeling method in which nodes are defined as stations, and train service routes are considered as edges [60]. Due to its ability to describe the dynamic service network of public transportation systems based on binary relationships between nodes and services, P-Space has been widely applied in the analysis of urban and ICTS [61,

62]. In this paper, the P-Space modeling method is used to describe the comprehensive intercity public transportation service network of urban agglomerations as a coupled system formed by two sub-networks of railways and roads, denoted as  $G = (G^{rail}, G^{road})$ . Here,  $G^{rail} = (V^{rail}, E^{rail})$  represents the railway sub-network, and  $G^{road} = (V^{road}, E^{road})$  represents the road sub-network.  $V^{rail}$  and  $V^{road}$  respectively denote the node sets of  $G^{rail}$  and  $G^{road}$ , while  $E^{rail}$  and  $E^{road}$  respectively denote the link sets within  $G^{rail}$  and  $G^{road}$ . In each sub-network, nodes represent train stations/long-distance bus stations that can provide intercity travel services, and if two nodes are adjacent stopping points of the same train, there is a link between the two nodes.

### 2.1.2. Description of intercity mobile signaling OD data generating passenger flow network

Fig. 2 shows the process of mapping mobile signaling OD data to the transportation service network. As shown in Fig. 2, intercity traveler  $i$  needs to travel from city A to city B. If the traveler's starting point is within 3 km of the nearest train station o, the traveler's destination is also within 3 km of the nearest train station d, and there are service frequencies from station o to station d in the transportation service network, then we consider that the traveler has completed the journey from city A to city B by taking the transportation service from station o to station d. Thus, we have completed the mapping of mobile signaling OD data to the intercity transportation service network.

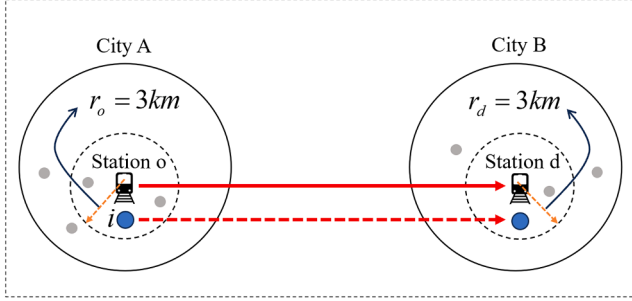


**Fig. 2.** Decision process of passenger flow network generated by mobile signaling od data.

## 2.2. Cascading failure modeling

### 2.2.1. Dual-factor capacity-loading model

In this paper, the classical capacity-loading model is used to describe the cascading failure process in transportation systems [33]. Generally, the capacity of network resources is limited, and the operational capability of websites is directly constrained by the frequency of operations and train capacity. Assuming the train capacity between link  $ij$  is  $C_{ij}^{train}$ , its value is equal to the product of the number of seats  $S_{ij}^{train}$ , the train frequency and the train capacity factor  $\alpha$ , as shown in Eq. (1). Here,  $\psi_{ij}^{train}$  represents the train frequency on the link within  $ij$ , and  $\alpha$  is capacity adjustment parameter, represents the number of passengers without seat reservations, its value is usually greater than 0.

$$C_{ij}^{train} = (1 + \alpha) \times \psi_{ij}^{train} \times S_{ij}^{train}, \alpha > 0 \quad (1)$$

For long-distance buses, considering the traffic safety risks brought by overload, the train capacity factor is usually equal to 0 in the actual operation process, and the vehicle capacity  $C_{ij}^{bus}$  is equal to the product of the number of seats  $S_{ij}^{bus}$  set by the train and the operating frequency  $\psi_{ij}^{bus}$  of the link within one day, that is:

$$C_{ij}^{bus} = \psi_{ij}^{bus} \times S_{ij}^{bus} \quad (2)$$

The load  $L_{ij}(t)$  of the train operating on link  $ij$  is the cumulative number of passengers who need to complete their journey through this line and have arrived at the station by time  $t$ . It has been found that an increase in passenger traffic can differentially exacerbate the magnitude

of cascading failures and the impact on network robustness [60,63], therefore, in this section, the load adjustment factor  $\beta$  is introduced to show the varying loads in the network, and the impacts of the load factor on the resilience of the network are investigated in the subsequent sections.

$$L_{ij}(t) = (1 + \beta) \times \left( L_{ij}(t_0) + \int_{t_0}^t A_{ij}(t) dt \right), \beta \geq 0 \quad (3)$$

Where  $L_{ij}(t_0)$  is the initial load,  $A_{ij}(t)$  is the number of passengers who arrive at station  $i$  at time  $t$  and need to travel through link  $ij$ .

According to the definitions of link capacity and load, we define the state of the link at time  $t$  as  $s_{ij}(t)$ . When the link capacity is greater than the load, the link is in a normal state, and  $s_{ij}(t) = 1$ , the link can continue to accommodate passengers in the network. When the link capacity is less than the load, the link exhibits an overloaded state, and  $s_{ij}(t) = 0$ , the link stops accepting new passengers in the network.

$$s_{ij}(t) = \begin{cases} 1, & \text{if } C_{ij} \geq L_{ij}(t) \\ 0, & \text{if } C_{ij} < L_{ij}(t) \end{cases} \quad (4)$$

### 2.2.2. Interrupt description

As shown in Fig. 3, suppose passenger  $s$  needs to travel from city A to city B. For passengers traveling intercity by public transportation, all the train stations and long-distance bus stations in the departure city A collectively form the set of candidate departure stations for passenger  $s$ , and similarly, all the train and long-distance bus stations in the destination city B collectively form the set of candidate destination stations for passenger  $s$ . Passengers will determine the most suitable route based on factors such as the distance between their location and the stations, train schedules, ticket prices, and so on.

When the train station  $i$  in city A is disrupted, passengers who originally needed to depart from station  $i$  will have to search for feasible paths to meet their travel needs. In this process, we designed two transfer scenarios: intra-city transfers and inter-city transfers. (1) Intra-city transfers include transfers at train stations and bus stations within the same city. Passengers first determine whether there are direct train services from City A to City B. If such services exist, they will use them to reach City B. If not, passengers need to check for direct bus services from City A to City B. If available, they will take the bus to City B. (2) If intra-city transfer does not meet the travel needs of passengers, they will consider inter-city transfers, which involve traveling from City A to City C via a station in City A, and then from City C to the destination City B through a station in City C. Given people's aversion to delays and

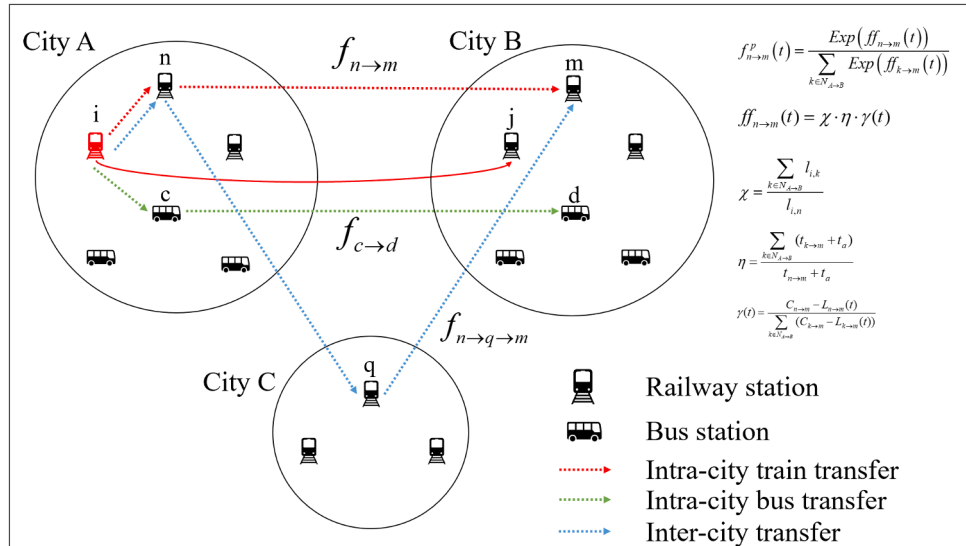


**Fig. 3.** After the attack on train station  $i$ , a schematic diagram of the shifting passenger flow paths.

inconveniences caused by transfers, this paper stipulates that passengers may only transit through one intermediate city for inter-city transfers.

When multiple viable routes are available during the transfer process, we will consider factors such as the distance to transfer stations, travel preferences, and time costs to quantify the probability of passengers choosing a particular route. Below, we provide specific allocation rules for passenger flow in both intra-city and inter-city transfer scenarios.

- Scenario 1: Intra-city transfer

If there is still a direct route from City A to City B after the interruption at the train station  $i$ , the detailed passenger flow assignment policy is as follows.

**Step1.** Determine the set of effective paths to be selected, give the method of calculating the passenger mobility at the station level. For passenger  $s(A \rightarrow B)$ , take the train station point  $i$  as the center of the circle and look around for the closest train station point  $n(n \in A, n \neq i)$ , determine whether passing through this station can generate an effective path  $f_{n \rightarrow m}$  to reach the station  $m$  in city B ( $m \in B$ , if multiple stations in city B can be reached by starting from  $n$ , the station closest to station  $j$  is taken as the end point of the path), and assume the probability of his/her exit through  $f_{n \rightarrow m}$  is  $f_{n \rightarrow m}^p(t)$ . The formula is shown in Eq. (5), which is a polynomial destination choice model, which has been developed and validated by some scholars [64] and has been widely used in transportation trip selection [65]. Until all nodes except  $i$  in city A are judged, the set of effective paths to be selected  $F_{A \rightarrow B}$  and the set of relocation sites to be selected  $N_{A \rightarrow B}$  are formed.

If no train station exists in city A that can reach city B, the travel behavior is carried out through the bus station, and the path selection method is the same as before.

$$f_{n \rightarrow m}^p(t) = \frac{\text{Exp}(ff_{n \rightarrow m}(t))}{\sum_{k \in N_{A \rightarrow B}} \text{Exp}(ff_{k \rightarrow m}(t))} \quad (5)$$

where  $ff_{n \rightarrow m}(t)$  is a spatial-temporal influence factor characterizing the ability of passenger flow at station  $i$  to be relocated to an effective path, calculated as shown in Eq. (6), where  $l_{i,n}$  is the distance between nodes  $i$ ,  $n$ , and  $t_{n \rightarrow m}$  is the travel time of the passenger on path  $f_{n \rightarrow m}$ .

$$ff_{n \rightarrow m}(t) = \chi \cdot \eta \cdot \gamma(t) \quad (6)$$

With

$$\chi = \frac{\sum_{k \in N_{A \rightarrow B}} l_{i,k}}{l_{i,n}} \quad (7)$$

$$\eta = \frac{\sum_{k \in N_{A \rightarrow B}} (t_{k \rightarrow m} + t_a)}{t_{n \rightarrow m} + t_a} \quad (8)$$

$$\gamma(t) = \frac{C_{n \rightarrow m} - L_{n \rightarrow m}(t)}{\sum_{k \in N_{A \rightarrow B}} (C_{k \rightarrow m} - L_{k \rightarrow m}(t))} \quad (9)$$

**Step2.** Node Route Assignment. As shown in Eq. (10),  $RFF_{n \rightarrow m|i \rightarrow B}(t)$  is the traffic  $FF_{i \rightarrow B}$  redistributed on path  $f_{n \rightarrow m}$  from site  $i$  to city B.

$$RFF_{n \rightarrow m|i \rightarrow B}(t) = \theta \cdot \min[FF_{i \rightarrow B} \times f_{n \rightarrow m}^p(t), C_{n \rightarrow m} - L_{n \rightarrow m}(t)] \quad (10)$$

$$\theta = \min \left[ \left( \frac{T_{n \rightarrow m}^{\text{original}}}{T_{n \rightarrow m}^{\text{now}}} \right)^{\xi}, 1 \right], 0 \leq \xi \leq 1 \quad (11)$$

In order to study the impact of passengers' choice tendency on network resilience, a passenger's time sensitivity factor  $\xi$  is defined here to characterize the passenger's sensitivity to travel time, when  $\xi = 0$ , it characterizes the passenger's time sensitivity to 0, the passenger doesn't

care at all about the loss of time cost due to transferring and interchanging, and when  $\xi = 1$ , it indicates that the passenger's time sensitivity reaches the maximum, the passenger's transferring behavior is maximized by the effect of the delayed time, and the larger the  $\xi$ , the greater is the effect of the delayed time on the passenger's transferring behavior.

- Scenario 2: Inter-city transfer

After the interruption at the train station point  $i$ , if there is no direct path from city A to city B, the traveler is assumed to transit to city B via city C. The detailed passenger flow assignment strategy is as follows.

**Step1.** Determine the set of effective paths to be selected, give the method of calculating the passenger mobility at station level. For passenger  $s(A \rightarrow C \rightarrow B)$ , take station  $i$  as the center of the circle, find the closest station  $n(n \in A, n \neq i)$  in the surrounding area, and find station  $q$  in city C among the stations directly connected to station  $n$ , so that it satisfies the requirement of being able to reach station  $m$  in city B through station  $q$ .

As a result, a valid path  $f_{n \rightarrow q \rightarrow m}$  is generated from City A to City B station  $m$  via City C (if multiple stations in City B can be reached from  $q$ , the closest station to station  $j$  is taken as the end point of the path), and the probability of traveling through  $f_{n \rightarrow q \rightarrow m}$  is assumed to be  $f_{n \rightarrow q \rightarrow m}^p(t)$ , as shown in Eq. (12) until all nodes in City A other than  $i$  have been judged to form the set of valid paths to be selected  $F_{A \rightarrow C \rightarrow B}$ , the set of relocation stations to be selected  $N_{A \rightarrow C}$ , and the set of transit stations to be selected  $N_{C \rightarrow B}$ .

$$f_{n \rightarrow q \rightarrow m}^p(t) = \frac{\text{Exp}(ff_{n \rightarrow q \rightarrow m}(t))}{\sum_{f_{o \rightarrow k \rightarrow m} \in F_{A \rightarrow C \rightarrow B}} \text{Exp}(ff_{o \rightarrow k \rightarrow m}(t))} \quad (12)$$

Where  $ff_{n \rightarrow q \rightarrow m}(t)$  is a spatial-temporal influence factor that characterizes the ability of passenger flow at station  $i$  to be relocated to an effective path, and is calculated as shown in Eq. (13), where  $l_{i,n}$  is the distance between nodes  $i, n$ ,  $t_{n \rightarrow q}$  is the travel time of the passenger on the path  $f_{n \rightarrow q}$ , and  $t_a$  is the waiting time of the passenger in transit at the transit station.

$$ff_{n \rightarrow q \rightarrow m}(t) = \chi \cdot \eta \cdot \gamma(t) \quad (13)$$

With

$$\chi = \frac{\sum_{o \in N_{A \rightarrow C}} l_{i,o}}{l_{i,n}} \quad (14)$$

$$\eta = \frac{\sum_{o \in N_{A \rightarrow C}} (t_{o \rightarrow k} + t_a + t_{k \rightarrow m})}{t_{n \rightarrow q} + t_a + t_{q \rightarrow m}} \quad (15)$$

$$\gamma(t) = \frac{\min[C_{n \rightarrow q} - L_{n \rightarrow q}(t), C_{q \rightarrow m} - L_{q \rightarrow m}(t)]}{\sum_{k \in N_{C \rightarrow B}} \min[C_{n \rightarrow k} - L_{n \rightarrow k}(t), C_{k \rightarrow m} - L_{k \rightarrow m}(t)]} \quad (16)$$

**Step2.** Node route assignment. As shown in Eq. (17),  $RFF_{n \rightarrow q \rightarrow m|i \rightarrow B}$  redistributes the traffic  $FF_{i \rightarrow B}$  from site  $i$  to city B to the traffic on path  $f_{n \rightarrow q \rightarrow m}$ .

$$RFF_{n \rightarrow q \rightarrow m|i \rightarrow B}(t) = \theta \cdot \min[FF_{i \rightarrow B} \times f_{n \rightarrow q \rightarrow m}^p(t), C_{n \rightarrow q} - L_{n \rightarrow q}(t), C_{q \rightarrow m} - L_{q \rightarrow m}(t)] \quad (17)$$

with

$$\theta = \min \left[ \left( \frac{T_{n \rightarrow m}^{\text{original}}}{T_{n \rightarrow m}^{\text{now}}} \right)^{\xi}, 1 \right], 0 \leq \xi \leq 1 \quad (18)$$

### 2.3. Assessment of resilience

#### 2.3.1. Network performance indicators

To assess the capacity of transportation networks to serve passengers and the changes in actual service levels in the traffic system due to disruptions, this paper proposes corresponding performance indicators for individual passenger service levels and overall system supply capacity. At the passenger level, the current service level of the network is characterized by calculating the effective transfer ratio of passengers during disruption events. At the system supply level, the relative service capacity indicator of the network is introduced to represent the supply capability of the transportation system.

##### (1) Passenger service indicator

$$f_p = \frac{\sum \delta(i)}{N_f^{\text{number}}}, i \in N_f \quad (19)$$

Scholars have utilized the passenger transfer rate during disruption events to assess network performance [66]. We follow this method to construct a passenger service level indicator. As shown in Eq. (19),  $f_p$  represents the proportion of passengers successfully transferred to a designated destination through the transportation system during a disruption event, reflecting the transportation network's ability to serve passengers in emergencies.  $N_f$  represents the set of passengers with demand for travel on that day in the transportation network, while  $N_f^{\text{number}}$  indicates the total number of passengers with travel demand in the transportation network for that day.  $\delta(i)$  is a state function that characterizes whether the transfer of traveler  $i$  is successful or not, and if traveler  $i$  is able to be transferred to the destination through the transportation service network,  $\delta(i) = 1$ , and vice versa,  $\delta(i) = 0$ .

##### (2) System service indicator

Compared to the traditional approach of using accessibility as a measure of transportation network performance, system service indicators designed based on travel time and service frequency can more accurately reflect the supply level of the transportation network [60]. This paper further refines this indicator to construct a service capacity indicator  $f_s$  for transportation systems, as shown in Eq. (20).

$$f_s = \frac{P^{\text{Interrupt}}}{P^{\text{normal}}} \quad (20)$$

with

$$P = \frac{1}{n(n-1)} \sum_{i \neq j \in G} \frac{\psi_{ij} \times S_{ij}}{t_{ij}} \quad (21)$$

In this case,  $P^{\text{Interrupt}}$  represents the performance of the system after an interruption, while  $P^{\text{normal}}$  represents the performance of the system under normal conditions.  $n$  represents the number of nodes in network  $G$ ,  $t_{ij}$  represents the commuting time between node  $i$  and node  $j$ ,  $\psi_{ij}$  represents the daily train frequency on route  $ij$ , and  $S_{ij}$  represents the number of seats available on the train.

#### 2.3.2. Resilience measurement metrics

Based on the understanding of network resilience, scholars employ various methods to assess it. Some define resilience as the ability to recover critical functions and adapt after destructive events [67], while others advocate expressing resilience as the integral of a system's critical functions over time [68]. In this study, we align with the mainstream view in the transportation sector [69–72], defining network resilience as the cumulative loss of performance during the damage and recovery process within the resilience cycle. Fig. 4 illustrates the process of

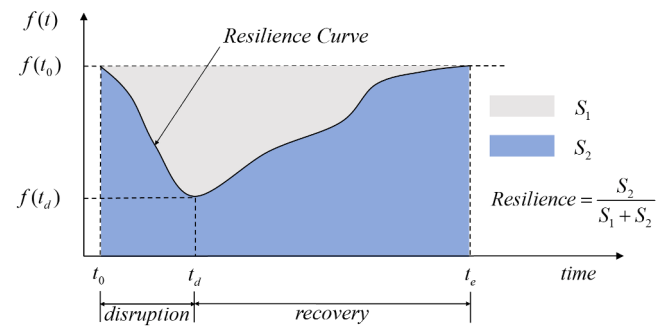


Fig. 4. Illustration of resilience index calculation based on network performance variation curves.

calculating resilience indicators based on network performance change curves, emphasizing a comprehensive focus on system damage, recovery, and adaptation processes.

As shown in Fig. 4, the network's performance declines continuously after receiving a shock at time  $t_0$ . After reaching its lowest point at time  $t_d$ , the network performance gradually increases as the recovery process progresses, until it is fully restored at time  $t_e$ . We define network resilience as the cumulative area ratio of the network performance from the interruption to the end of the recovery phase, as specified in Formula (22).

$$R = \frac{S_2}{S_1 + S_2} = \frac{\int_{t_0}^{t_e} f(t) dt}{f(t_0)(t_e - t_0)} \quad (22)$$

In this context,  $f(t)$  represents the performance function, indicating the network performance metric value at time  $t$ , while  $f(t_0)$  denotes the initial performance value of the network.

Based on the network performance indicators defined in Section 2.3.1, the calculation methods for two network resilience indicators are provided, as shown in formulas (23) and (24). Here,  $R_p$  represents passenger service resilience, which reflects the level of service provided to passengers by the transportation network during damage and recovery processes.  $R_s$  denotes system service resilience, indicating the overall supply capability of transportation infrastructure during network damage and recovery.  $f_p(t)$  is the passenger service indicator at time  $t$ , calculated as shown in formula (19).  $f_s(t)$  is the system service indicator at time  $t$ , calculated as shown in formula (20).

$$R_p = \frac{\int_{t_0}^{t_e} f_p(t) dt}{f_p(t_0)(t_e - t_0)} \quad (23)$$

$$R_s = \frac{\int_{t_0}^{t_e} f_s(t) dt}{f_s(t_0)(t_e - t_0)} \quad (24)$$

### 3. Case study and results

Based on the intercity transportation elasticity simulation framework built in Section 2, a MATLAB program was used to simulate and analyze the ICTS in the Beijing-Tianjin-Hebei region. Firstly, we construct an intercity comprehensive transportation network composed of timetable data and mobile signaling origin-destination (OD) data in Section 3.1. Secondly, we define  $\xi = 0$ ,  $\alpha = 0.1$ ,  $\beta = 1$  and investigate the resilience of an integrated intercity public transportation network in both single and continuous attack scenarios in Section 3.2. Additionally, we analyze the impact of passenger choice behavior on the network in Section 3.3. Finally, we examine the resilience changes caused by the supply-demand relationship in the transportation network in detail in Section 3.4. Meanwhile, we make the following assumptions:

- 1) After an interruption event occurs, passengers need to transfer from the faulty station to the destination station within the city. Considering the speed of urban transportation vehicles and the waiting time for transfers [73], we assume that the time loss for passengers to complete a transfer is  $t_a = 1h$ .
- 2) This study does not consider the influence of rescue operations in the simulation process. For links or nodes that are attacked, we remove them from the network. For overloaded lines caused by cascading effects, we consider them temporarily disabled and assume that their functionality will be restored once the overloaded passengers are evacuated.

The total number of experiment calculations completed was 10,079,472 times (attacking one node, waiting for load redistribution to finish, and calculating relevant indicators constitute one simulation), taking approximately 280 h. The simulation results were obtained running on a platform with a 13th Gen Intel(R) Core (TM) i7-13,700 K 16-Core Processor 3.40 GHz and 64GB memory.

### 3.1. Simulation scenarios description

#### 3.1.1. Data description

This study utilized mobile signaling data, transportation station coordinates, and train timetable data in the Beijing-Tianjin-Hebei region. The mobile signaling data was provided by China Mobile, collected on September 27, 2021, and comprised a total of 3454,582 records of resident travel data, describing intercity travel activities within the BTH-UA. The mobile signaling data illustrates the distribution of intercity resident travel in the Beijing-Tianjin-Hebei region, as shown in Fig. 5(a), and the hourly distribution is depicted in Fig. 5(e). Additionally, the transportation station coordinates were obtained from Baidu Maps, while the train timetable data was sourced from China Railway, and the bus timetable data was obtained from a long-distance bus ticket platform serving the Beijing-Tianjin-Hebei region. The railway network, as shown in Fig. 5(b), includes a total of 156 train stations, and the road network, as depicted in Fig. 5(c), encompasses 165 long-distance bus stations.

#### 3.1.2. Construction of intercity comprehensive transportation network in BTH-UA

As shown in Fig. 6, the intercity comprehensive public transportation network for the BTH-UA consists of three parts: infrastructure network, transportation service network, and passenger flow network. Fig. 6(a) displays the intercity infrastructure network within the BTH-UA, including train stations, long-distance bus stations, railway networks, and road networks. Fig. 6(b) presents the intercity comprehensive public transportation service network for the BTH-UA, comprising 156 train stations, 165 long-distance bus stations, 700 railway transportation service links, and 1223 bus transportation service links. Fig. 6(c) illustrates the intercity passenger flow network derived from mobile signaling data, where node colors represent the respective cities, link colors correspond to the colors of the departure stations, and thicker links indicate higher passenger travel demand along the routes.

#### 3.1.3. Attack and recovery strategy

When simulating network disruptions, we attack or restore the network by individually removing or adding nodes. When a node in the network is attacked, we assume it becomes incapacitated, resulting in all links connected to that node failing, preventing passengers from using that node and its associated links for transport. Once an attacked node in the network is restored, we reactivate the transport functions of that node and its connecting links, allowing passengers to travel through that node and its associated links again. When determining the order of attacks on nodes in the network, we designed a target attack strategy based on passenger flow weighting. At the same time, to explore the impact of different recovery strategies on network resilience, we referenced current research by scholars and selected four mainstream recovery strategies for comparison: degree-based recovery strategy, passenger flow-based recovery strategy, betweenness-based recovery strategy, and random recovery strategy [72,74,75]. A detailed explanation of different strategies is as follows.

**Target attack strategy based on passenger flow:** During an attack, we adopt a targeted approach, sorting nodes based on passenger flow from highest to lowest and sequentially removing them.

**Degree priority recovery strategy:** Nodes are arranged in descending

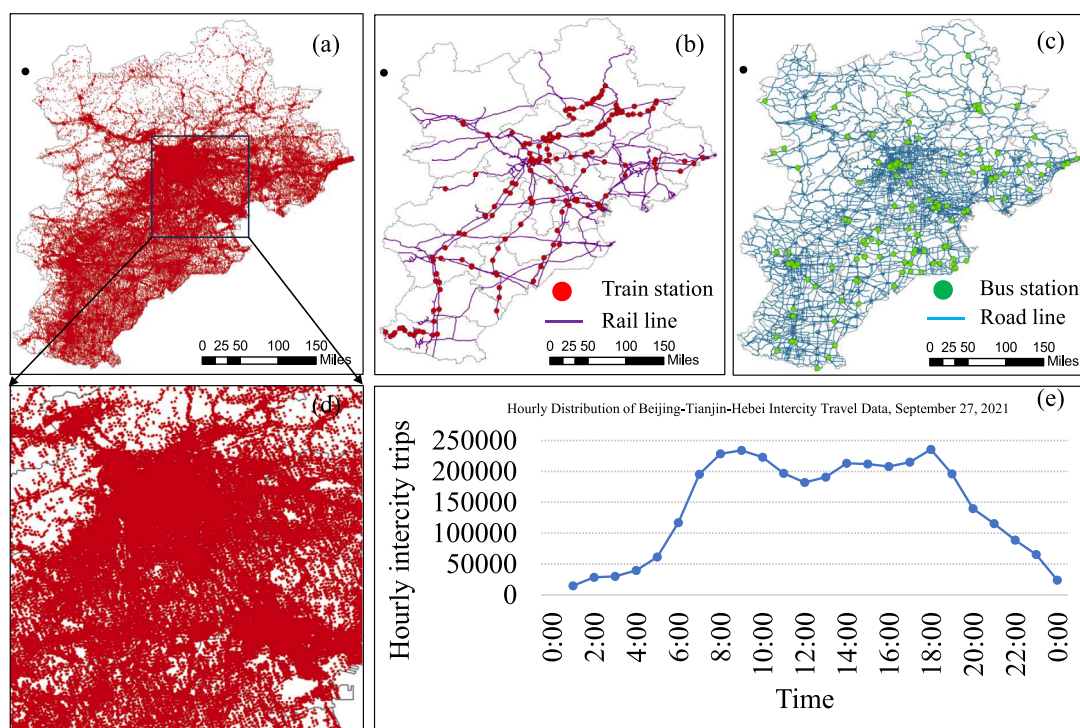
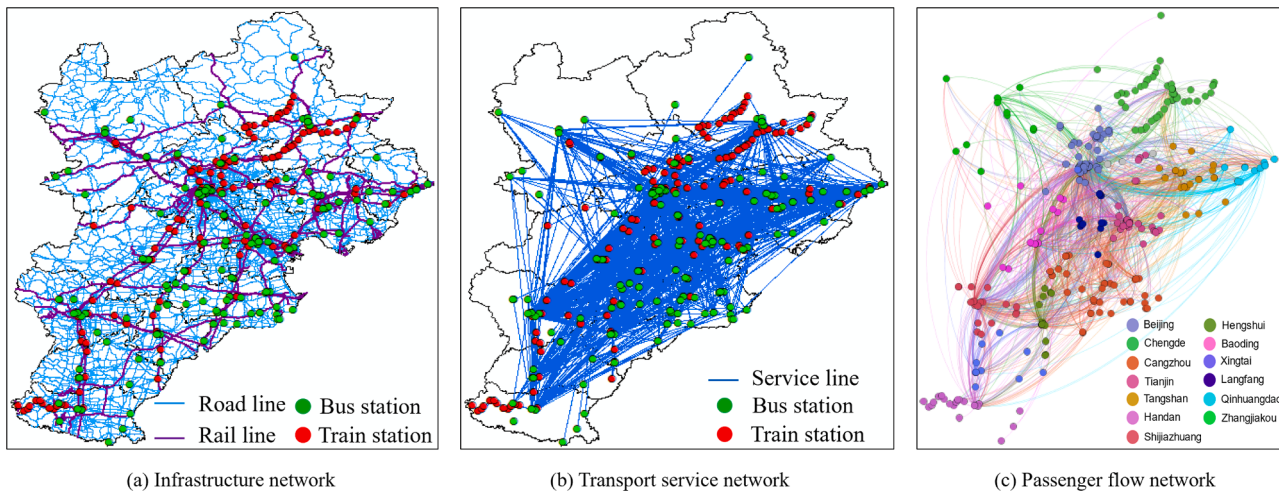


Fig. 5. ICTS data display of BTH-UA.



**Fig. 6.** Intercity passenger flow mapping based on cell phone signaling OD data and transportation service network.

order based on degree, and then recovered sequentially.

Passenger flow priority recovery strategy: Nodes are arranged in descending order based on passenger flow, and then recovered sequentially.

Node betweenness recovery strategy: Nodes are arranged in descending order based on betweenness, and then recovered sequentially.

Random recovery strategy: A random sequence of recovery is generated, and nodes are recovered in that order. Notably, to reduce the uncertainty of random recovery, and to enhance the readability and comparability of results, we generated 1000 random sequences and averaged the simulation results to produce the final random recovery curve.

### 3.2. Network resilience in target attack scenarios

#### 3.2.1. Comparison of CTS and RTS after attacking single node

This section takes Beijing Station as an example to show the evacuation path of passenger flow after a single station attack. Among them, Fig. 7 is RTS and Fig. 8 is CTS. As shown in Fig. 7(b), after the failure of Beijing Station, passengers who originally need to travel through Beijing Station for intercity travel first look for a train station within the same city where they can reach their destination and arrive at their destination through this station. When the capacity of the railway station in the same city cannot meet the demand for passenger flow, passengers will adopt the mode of intercity transfer. As shown in Fig. 7(c), passengers

will first arrive at the intermediate transfer city from Beijing and then arrive at the destination city through the intermediate transfer city. Fig. 8(b) shows the route that passengers in CTS take to reach their destination through the same city train station after the Beijing station is defunct. Fig. 8(c) shows the route for passengers in CTS to reach their destination through the same city bus station after the Beijing station is defunct. Observing Fig. 8(d), it can be found that no passengers are transported by intercity transfer in CTS, which indicates that the intra-city transfer service in CTS has been able to meet the passenger transfer demand caused by the failure of Beijing Station. By comparing Figs. 7 and 8, it can be seen that all evacuated passengers in CTS can reach their destination through intra-city transfer, while passengers in RTS can't meet their needs due to intra-city transfer, so some passengers need to reach their destination through inter-city transfer. This shows that in the case of traffic disruption, the integrated transportation system provides passengers with more adequate intra-city transfer service capacity, so that passengers avoid complex inter-city travel organization and more transit delay losses.

#### 3.2.2. Comparison of CTS and RTS under continuous attacks

This section analyzes the resilience performance of RTS and CTS networks under continuous attacks. During an attack, we adopt a targeted approach, sorting nodes based on passenger flow from highest to lowest and sequentially removing them.

Fig. 9 illustrates the distribution of links in the RTS network during continuous attacks. It can be observed that the number of links in the

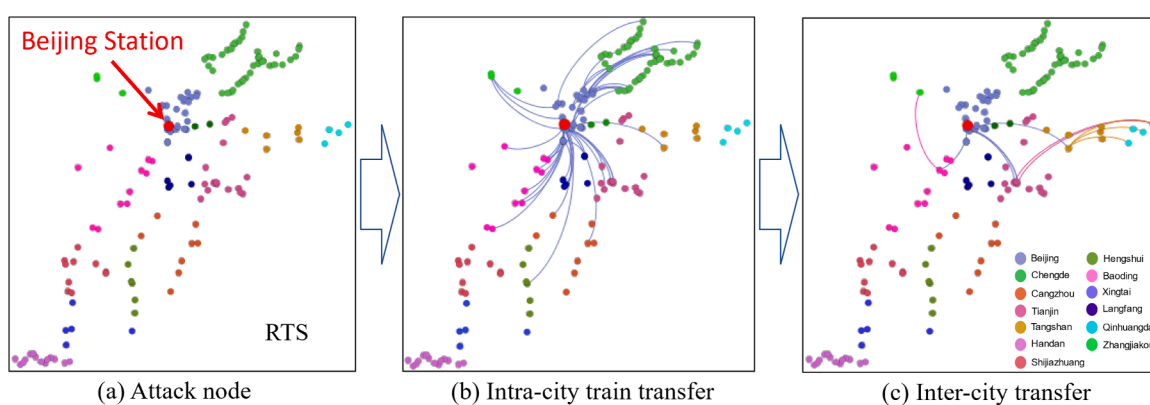


**Fig. 7.** illustrates the alternative routes that intercity travelers must take through other stations after the Beijing station was attacked in RTS. Each node represents a station, and the color of the node indicates its associated city. Figure (a) shows the original railway network; figure (b) depicts the paths taken by intra-city transfers to reach their destination; and figure (c) outlines the routes for those using inter-city transfers to arrive at their destinations.

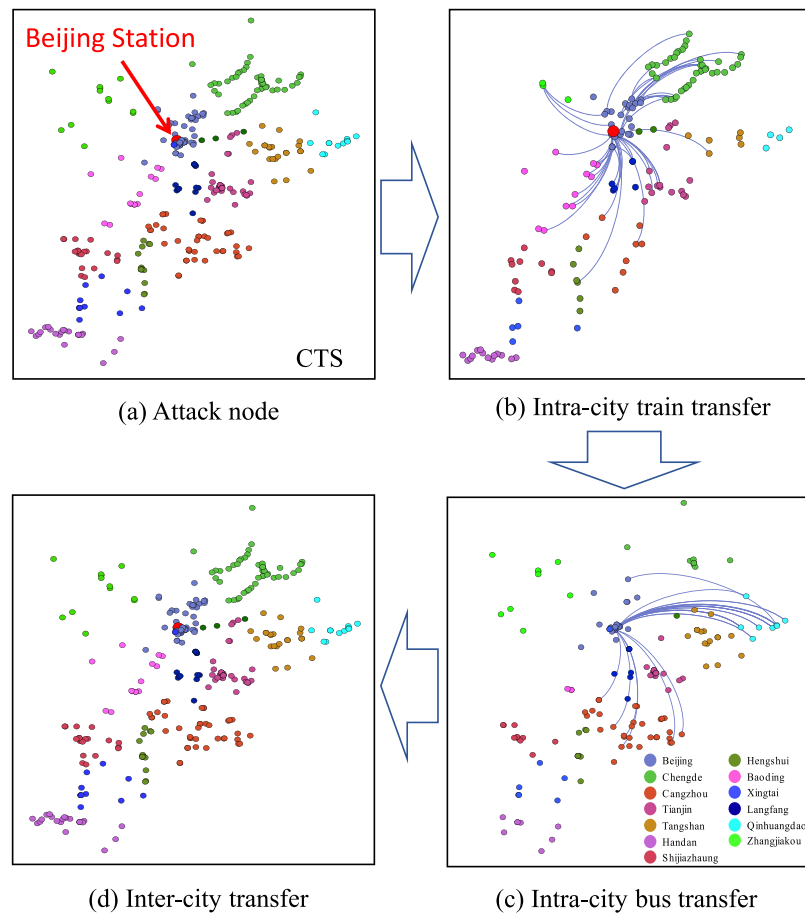


**Fig. 8.** illustrates the alternative routes intercity passengers must take through other stations after the attack on Beijing Station in the CTS. Each node represents a station, and the color of the node indicates its associated city. Figure (a) shows the integrated transport network consisting of rail and road; figure (b) depicts the route to the destination via train transfers within the city; figure (c) shows the route to the destination via bus transfers within the city; and figure (d) indicates that no passengers need to use inter-city transfers to reach their destination.

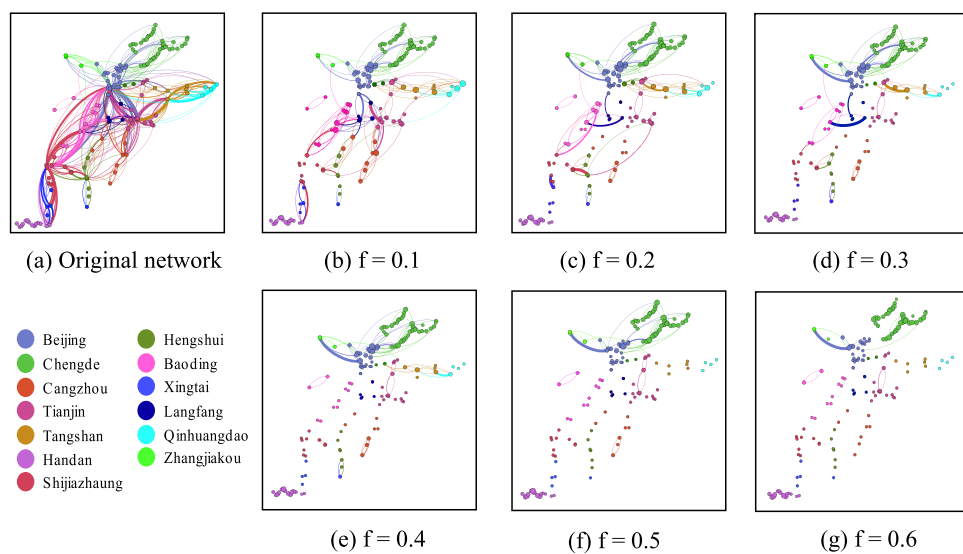


**Fig. 9.** The distribution of passenger traffic during the sequential removal of components in RTS according to node weights is shown. Thicker lines in the graph indicate more passenger traffic on the link.  $f$  is the percentage of nodes removed.

network gradually decreases as the proportion of attacked nodes increases. When the proportion of attacked nodes reaches 10% ( $f = 0.1$ ), widespread link interruptions occur in the network. As more

components are removed, the number of network interruptions increases. When the proportion of attacked nodes reaches 60% ( $f = 0.6$ ), almost all links in the network are disrupted, with only a few remaining

operational.

Fig. 10 shows the distribution of links in the CTS network during continuous attacks. To demonstrate the process of passenger flow redistribution more clearly, we depict the bus subsystem (BSS) and railway subsystem (RSS) separately. As the proportion of removed nodes increases, the proportion of link interruptions in the network also increases. When  $f = 0.6$ , almost all links in the RSS are completely disrupted.

By comparing Figs. 9 and 10, we find that there are significant differences in the distribution of passenger flows between CTS and RTS networks during component removal. Compared to RTS, the flow distribution in CTS is more evenly distributed, and the number of heavily loaded links is less. This is because BSS supports the flow of RSS, creating a network structure with more capacity space, which exhibits higher robustness against continuous attacks.

To explore the impact of different recovery strategies on network resilience under various transportation systems, we selected four recovery strategies for comparison: degree-based recovery strategy, passenger flow-based recovery strategy, betweenness-based recovery strategy, and random recovery strategy. Fig. 11 shows the resilience curves of the network under the four recovery strategies, illustrating the transition from being attacked to final recovery. The X-axis represents

the number of nodes removed or recovered, while the Y-axis indicates network performance. The calculations of network resilience in various scenarios are presented in Table 1.

Observing Fig. 11 (a-d) and Table 1 reveals that the process of network attack and recovery forms a triangular resilience curve. The CTS system generally performs better than the RTS during both attack and recovery. Meanwhile, during recovery based on the degree value strategy, the RTS demonstrated better resilience in the system service levels ( $f_s$  and  $R_s$ ) compared to CTS. This finding contradicts common assumptions and highlights the significant impact of recovery strategies on network restoration efficiency during disaster recovery phases. The random recovery strategy performed the worst, notably in the RTS. Additionally, the effects of different recovery strategies on resilience in the CTS and RTS systems vary. For instance, the passenger flow recovery strategy performed best in the CTS but was least effective in the RTS (Fig. 11(a) and (c)). Furthermore, the impact of recovery strategies on passenger service indicator ( $f_p$ ) and system service indicator ( $f_s$ ) differs. In the CTS, the best recovery strategy for passenger service resilience is the passenger flow recovery strategy (Fig. 11(a)), while for system service resilience, the best is the node betweenness recovery strategy (Fig. 11(b)). This may be due to stations with high passenger flow enabling large groups of travelers to transfer quickly, whereas node

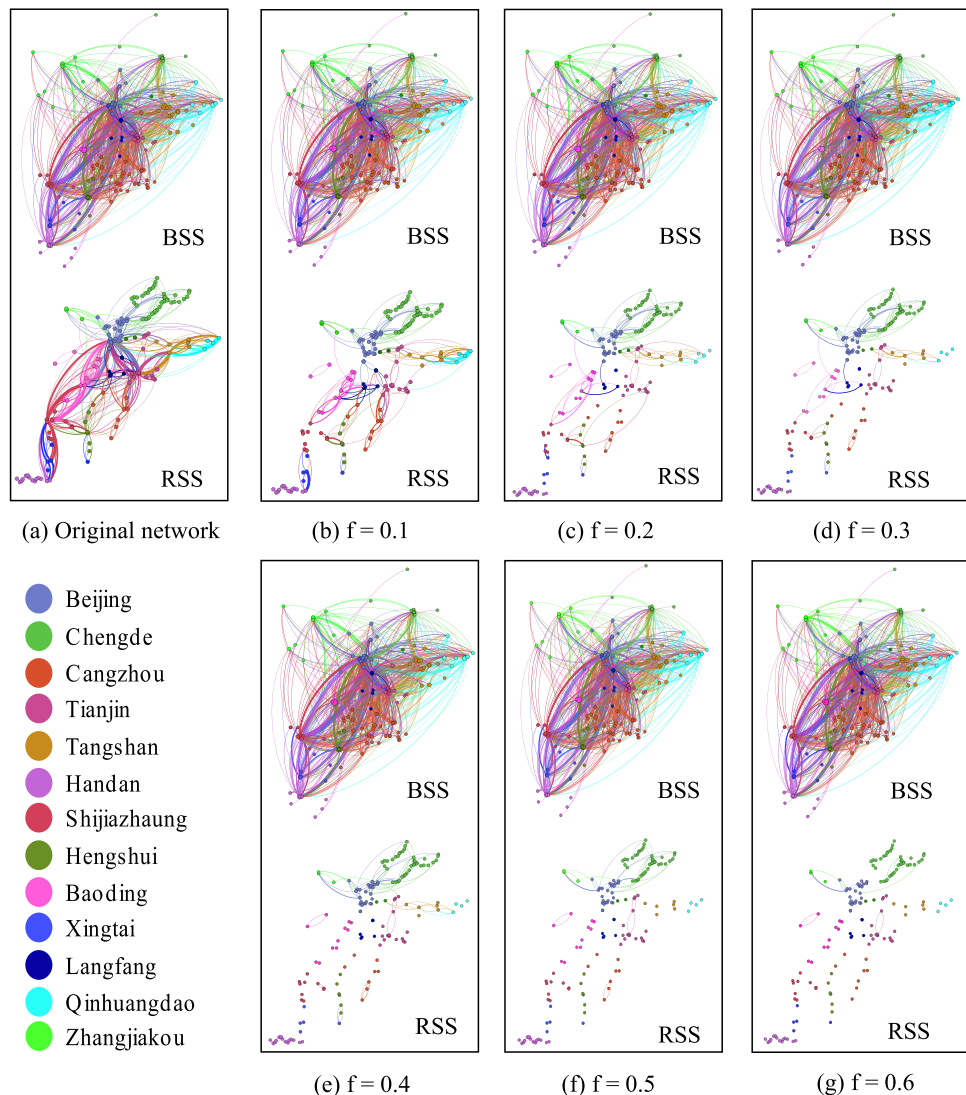


**Fig. 10.** The distribution of passenger flows during the sequential removal of components in CTS according to node weights is shown. RSS and BSS are plotted separately to better demonstrate the role of the road network in undertaking passenger flows on the rail network. Thicker lines in the graph indicate more passenger flows on the link.  $f$  is the proportion of nodes removed.

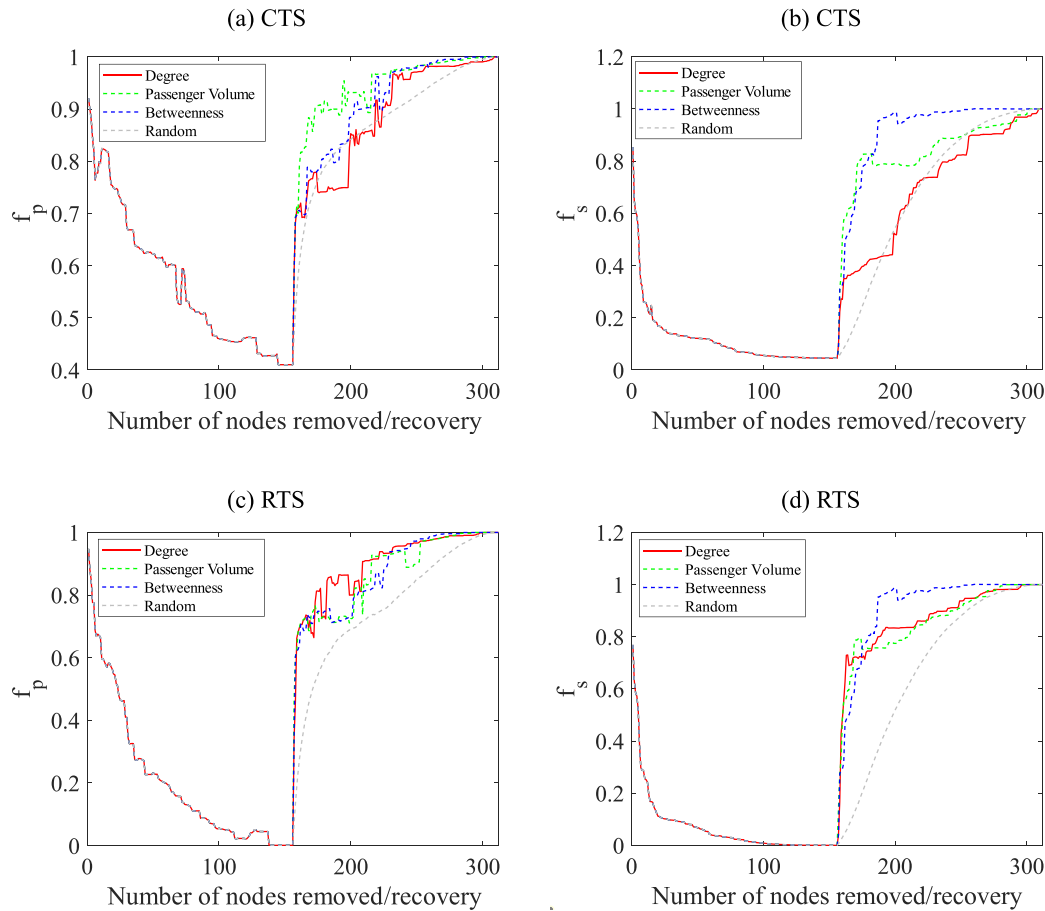


**Fig. 11.** Resilience curves of CTS and RTS under different recovery strategies.

**Table 1**  
Calculation results of network resilience in four recovery scenarios.

Recovery strategies	CTS		RTS	
	RA	RB	RA	RB
Degree	0.727	0.412	0.552	0.468
Passenger Volume	0.755	0.479	0.539	0.462
Betweenness	0.740	0.515	0.539	0.490
Random	0.722	0.408	0.484	0.377

betweenness better reflects a station's connectivity to other components of the network. The recovery of high-betweenness nodes enhances overall connectivity, providing greater redundancy and leading to better

overall resilience.

In summary, the presence of multiple transport modes in integrated transportation systems generally offers travelers better alternative routes during interruption events, improving service capacity. Additionally, the choice of recovery strategies significantly affects the efficiency of network recovery. Therefore, different resilience optimization strategies should be selected for individual and system-level resilience goals.

### 3.3. Impact of passenger choice behavior on network resilience

This section keeps  $\alpha$  and  $\beta$  constant while varying the value of  $\xi$  to investigate the influence of passenger choice inclination on network resilience. Fig. 12 (a and b) illustrate the changes in network resilience

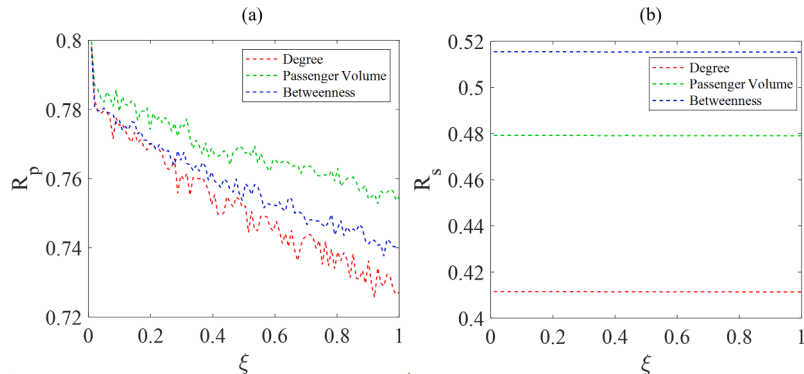


**Fig. 12.** The Impact of Passenger Choice Propensity on Network Resilience.

as the passenger sensitivity factor  $\xi$  is adjusted (starting from  $\xi=0$  and increasing by 0.01 with each calculation), under three different recovery strategies (degree priority recovery, passenger flow priority recovery, and betweenness centrality priority recovery).

As shown in Fig. 12(a), the passenger service resilience ( $R_p$ ) decreases gradually with the increase of  $\xi$  under three recovery strategies. The value of  $\xi$  reflects passengers' aversion to the losses caused by delays. As  $\xi$  increases, the passenger service resilience diminishes, indicating that when network disruptions occur, a greater concern for delays caused by transfers results in lower efficiency in transferring passenger flow after the transportation network is impacted. Initially, as  $\xi$  increases from 0, there is a noticeable jump in the decline of passenger service resilience, followed by a steady decline with certain fluctuations. This suggests that passengers' aversion to delays is negatively correlated with passenger service resilience, although not in a completely proportional manner, as it decreases amidst fluctuations. Observing Fig. 12(b), it is evident that changes in the  $\xi$  value do not affect the system service resilience ( $R_s$ ); passengers' sensitivity to delays does not impact the overall resilience of the network.

The above analysis provides guidance for network maintenance: under limited resources, if transportation system managers focus more

on facilitating the transfer of passengers affected by disruptions, they should aim to minimize the  $\xi$  value. This can be achieved by enhancing services and pricing to attract passengers, thereby reducing their sensitivity to travel time and improving the appeal of transportation services. Conversely, if managers prioritize the rapid recovery of the overall service capacity of the transportation system, they may relax their focus on individual passengers and concentrate on optimizing existing transportation capabilities.

#### 3.4. Impact of network supply-demand relationship on network resilience

$\alpha$  and  $\beta$  are control parameters that describe the supply and demand relationships of the transportation network in constructing the cascade failure model. This section examines how changes in  $\alpha$  and  $\beta$  values impact the relationship between network capacity and load, and subsequently, the network's resilience. Fig. 13 (a–f) illustrate the variations in network resilience as  $\alpha$  and  $\beta$  change (starting from 0 and increasing by 0.01 with each calculation) under three different recovery strategies: degree-priority recovery, passenger flow-priority recovery, and node betweenness-priority recovery.

$\alpha$  is a regulatory parameter that describes the supply capacity of a

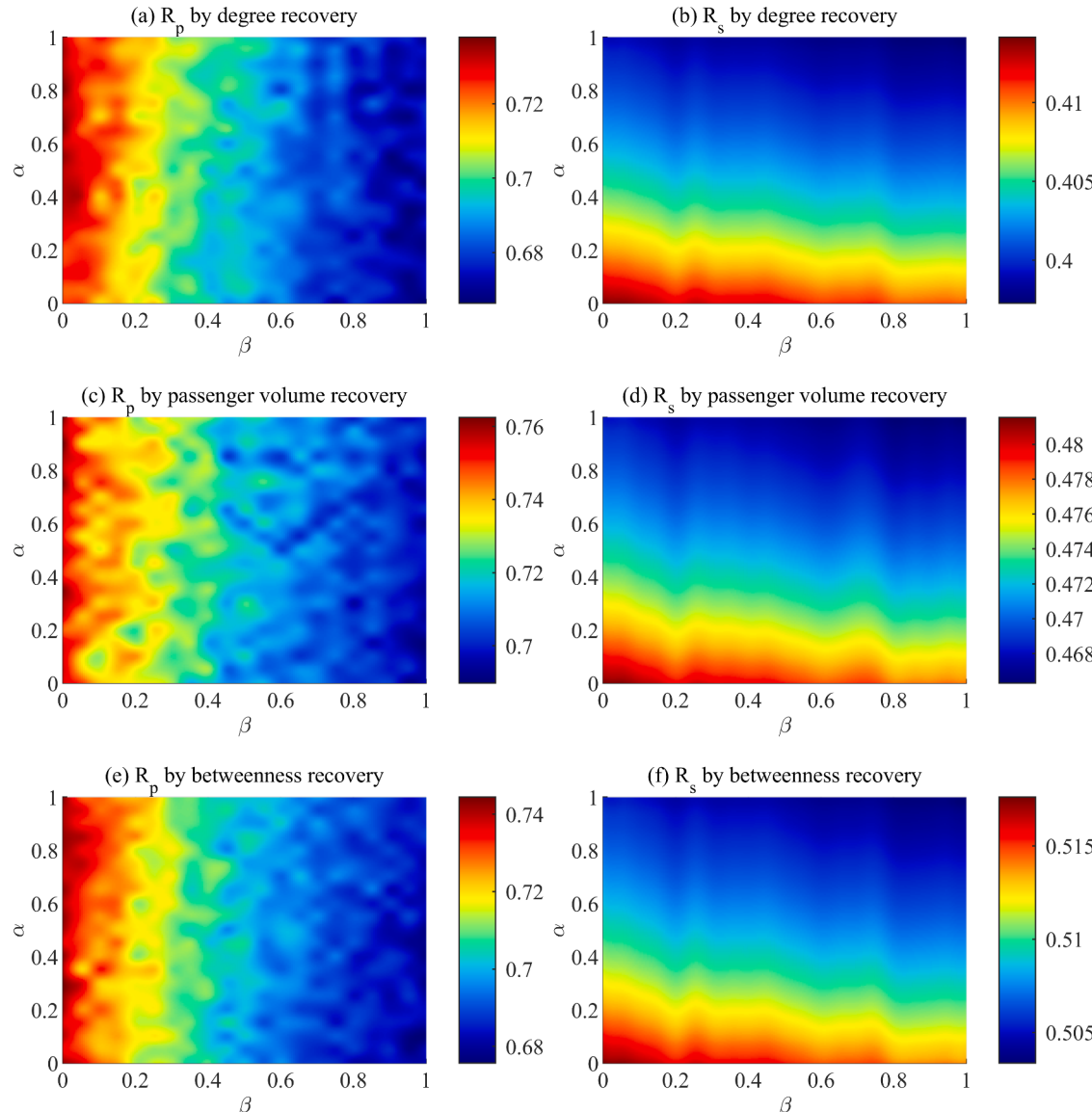


Fig. 13. Sensitivity analysis of capacity and load factor parameters.

transportation network, while  $\beta$  serves as a regulatory parameter for passenger flow demand. Under three recovery strategies, as illustrated in Fig. 13(a), (c), and (e), when  $\alpha$  remains constant, the passenger service resilience ( $R_p$ ) gradually decreases as  $\beta$  increases. This indicates that increased network load intensifies pressure on the transportation system, leading to a decline in the efficiency of passenger transfer during disruption events. When  $\beta$  is held constant,  $R_p$  does not exhibit a clear linear correlation with  $\alpha$ , showing instances where resilience suddenly increases or decreases in certain areas. This phenomenon varies in degree across different recovery strategies and  $\beta$  values, revealing a more complex pattern. As shown in Fig. 13(b), (d), and (f), the system service resilience ( $R_s$ ) exhibits a negative correlation with both  $\alpha$  and  $\beta$ , with  $\alpha$  having a greater impact on  $R_s$  than  $\beta$ . This suggests that the network-level system resilience is correlated with both the supply capacity of infrastructure and actual traffic demand. Increased load can lead to a reduction in the network's redundancy capacity, thereby diminishing system resilience. Moreover, greater supply capacity does not always translate to better outcomes; if the supply significantly exceeds transportation demand, increasing infrastructure supply poses substantial risks, resulting in poorer resilience during sustained disasters and recovery processes.

The differing impacts of  $\alpha$  and  $\beta$  on resilience highlight the necessity of approaching network resilience optimization from both supply and demand perspectives. In addition to building new stations and expanding lines to enhance network supply capacity, targeted adjustments to passenger flow load through changes in passenger distribution and travel guidance are crucial, especially when there is significant redundancy in network supply capacity.

## 4. Discussion

### 4.1. The advantages of resilience simulation model for ICTS

In Section 3.2, we simulated RTS and CTS separately and conducted a comparative analysis of their resilience performance under four recovery strategies: degree-priority recovery, passenger flow-priority recovery, betweenness-priority recovery, and random recovery. The results indicate that CTS, which considers both rail and road transport modes, generally demonstrates better resilience than RTS during disruption events. By analyzing passenger flow propagation paths during interruptions, we found that CTS's superior resilience compared to RTS is due to the existence of the road transport system, which allows affected passengers to choose direct routes to their destination cities. In contrast to the transit transport mode provided by RTS, road transport offers passengers greater route selection flexibility, enhancing the service capability of the transportation system, which is directly reflected in the improved system resilience. This finding is consistent with the existing understanding of long-distance traffic and urban traffic [32,60], and also indicates that there are certain commonalities between the resilience performance of urban agglomeration traffic and urban traffic. Additionally, appropriate recovery strategies significantly impact network efficiency. Under poor recovery strategies, the resilience of a single transport system may even surpass that of an integrated transport system. Moreover, the study found that during the ongoing failure of system components, the individual passenger resilience index and system service resilience index show different trends, indicating that individual service levels and system service capacity have distinct failure thresholds. It is crucial to adopt different resilience optimization and node recovery strategies when targeting both individual and system resilience optimization goals. In summary, the resilient simulation framework designed considering passenger choice behavior reveals the reasons why CTS exhibits better resilience than RTS from the bottom level and analyzes the system resilient characteristics under continuous target attack and different recovery strategies from the two levels of passenger demand and system supply, and more comprehensively

demonstrates the resilience evolution trend of traffic network under fault state.

When constructing the passenger route choice model, the parameter  $\xi$  was introduced to quantify passengers' sensitivity to travel time. In Section 3.3, we studied how passengers' choice tendencies affect network resilience by varying the value of  $\xi$ . The results showed that, at the individual level, passengers' choice tendencies significantly impact the network resilience index. The more sensitive passengers are to travel time, the lower the transfer efficiency of the transportation network will be, but this relationship is not entirely proportional; it declines gradually with fluctuations. This suggests that for network maintenance, if traffic system managers prioritize the transfer of passengers affected by disruptions, they should aim to minimize the  $\xi$  value, either by enhancing service quality or adjusting pricing to attract passengers, thereby reducing their travel time sensitivity and improving the attractiveness of transport services. Conversely, if managers focus on the rapid recovery of the overall service capacity of the transport system, they might relax their attention on individual passengers and instead emphasize optimizing existing transport capacity. Furthermore, simulation results suggest that passengers' choice tendencies have a much smaller impact on system service resilience, indicating that indicators designed solely from a system perspective may struggle to identify the influence of individual passenger levels on network resilience. The research also indicates that the individual resilience index we constructed can effectively capture fluctuations in traffic service level caused by changes in passenger factors.

In building the cascading failure model, a dual-parameter control method was introduced to adjust the supply-demand relationship in the transport network. Section 3.4 results reveal that both network capacity and load affect network resilience, and the impact of load parameters on network resilience varies under different network capacities. This finding not only supports existing conclusions that increased load can exacerbate the scale of cascading failures to varying degrees, hence affecting network resilience [64], but it also highlights the advantages of the dual-parameter control model. Compared to traditional methods which keep network load constant, the introduction of capacity parameters allows for the calibration of network capacity [38,39]. The addition of these two parameters enables more targeted adjustments to the network's supply-demand relationship and facilitates a deeper analysis of network resilience and its mechanisms. Analysis of the simulation results indicates that  $\alpha$  does not have a positive correlation with network resilience, reflecting the distinct characteristics of urban agglomeration transportation compared to urban transportation. The supply and demand relationship in intercity transportation is more complex and variable than that of urban transit. For instance, during traffic restrictions due to natural disasters, public health events, or terrorist attacks, the transportation network may exhibit significant redundancy (in such cases, increasing network supply will not enhance resilience). Conversely, a sharp increase in intercity travel demand during holidays can lead to a shortage of supply capacity. These characteristics underscore the urgency of conducting resilience analysis of intercity transportation systems using actual data rather than weighted network indicators. Moreover, the differing impacts of  $\alpha$  and  $\beta$  on resilience remind us that optimizing network resilience should address both supply and demand sides. In addition to constructing new stations and expanding routes to increase supply capacity, it is crucial to adjust network passenger loads through measures such as restructuring passenger flow and travel guidance, especially when there is considerable redundancy in supply capacity.

### 4.2. Take aways

The research findings provide insights into constructing resilient transportation systems: (1) Multi-modal integrated systems have strong accident resistance. When failures occur in the transportation system, more traffic measures should be implemented to alleviate the shift and

distribution of passenger flow caused by accidents. (2) After network disruption, appropriate transportation recovery strategies significantly impact the restoration of network service capacity, making it crucial to identify the optimal recovery sequence during damage to enhance network resilience. (3) Different resilience optimization objectives should lead to targeted network recovery strategies. In this study, the most effective recovery strategy for passenger service resilience is the passenger flow recovery strategy, while the best for system service resilience is based on node betweenness. (4) Passenger sensitivity to commuting time directly affects passenger service resilience but has a minimal impact on infrastructure supply resilience. Managers can reduce passenger sensitivity to travel time through services and pricing, thus enabling more flexible passenger movement within the network. (5) It is essential to timely develop corresponding resilience management methods for varying transportation supply-demand relationships to reduce the systemic resilience risks posed by fluctuations during disruptive events.

#### 4.3. Limitations

The framework proposed in this article helps to understand the interaction mechanism between passenger choice behavior and system service capacity. The combination of traveler perspective and infrastructure perspective provides a more open approach for analyzing the resilience of transportation networks in the system. However, this study also has certain limitations. Firstly, the mobile signaling data and timetable data used in the study were dated September 2021, and passenger travel conditions were inevitably affected by the COVID-19 pandemic. Secondly, the constructed transportation network only considers two modes of transportation: railways and highways. However, the intercity transportation modes in the real world are more diverse, and the transfer distribution of passenger flows during accidents will be more complex. Thirdly, although this study has designed multiple simulation scenarios including single/multiple transportation systems, single/continuous attacks, and intra-city/inter-city transfer distribution, further research on urban agglomeration transportation systems that include more scales and scenarios is still needed. In addition, the current focus on the resilience of urban agglomeration transportation systems is mostly in the qualitative analysis stage, and there is less research that quantitatively simulates the resilience of urban agglomeration transportation systems and analyzes the underlying mechanisms of resilience performance. Therefore, it is worth further exploring how to introduce more advanced research methods and fully utilize the massive intercity commuting data in the era of big data to study the resilience of urban agglomeration transportation systems, as well as how to further enhance the resilience of long-distance regional transportation networks represented by urban agglomerations through policy measures in future work.

#### 5. Conclusions

With the continuous expansion of China's urban agglomerations, various types of emergencies and natural disasters pose an increasingly serious threat to urban safety. During emergencies and natural disasters, intercity public transportation systems play a critical role in evacuating personnel, transporting disaster materials, and promoting post-disaster reconstruction. This article considers passenger choice and infrastructure carrying capacity to construct a resilience simulation framework for ICTS in urban agglomerations, aiming to provide new ideas and effective methods for evaluating the resilience of urban agglomeration transportation networks. Firstly, an actual passenger flow-weighted intercity comprehensive public transportation service network for urban agglomerations is constructed based on mobile signaling data, station location data, and train timetable data. Secondly, considering passenger route choice tendencies and infrastructure carrying capacity, a cascading failure model for ICTS in urban agglomerations is established

to simulate the changes in service performance of ICTS caused by traveler choice behavior during interruption events. Finally, taking the BTH-UA as a case study, the impacts of node recovery strategy, traveler choice tendencies, network capacity, and network load on the resilience of intercity public transportation systems are explored.

Research findings indicate that: (1) When a single site is compromised, the resilience of integrated systems and rail systems performs similarly. (2) During sustained deliberate attacks on networks, multi-modal transportation systems typically exhibit better resilience. During the network recovery process, the choice of appropriate restoration strategies can sometimes be more effective in enhancing system resilience than introducing new transportation connections. (3) Suitable restoration strategies significantly boost the resilience of transportation systems, particularly when aimed at different resilience optimization objectives. (4) In transportation disruption events, passenger choice tendencies can significantly impact the service efficiency of transportation systems; the more passengers prioritize travel time, the worse the service efficiency of the transportation system tends to be. (5) Passenger choice tendencies generally have little effect on the network resilience at the infrastructure supply level. (6) Changes in transportation supply capacity and travel demand both affect system resilience; an increase in travel demand can put the network under heavy load, and the resulting system risk may lead to poorer resilience during disasters.

#### CRediT authorship contribution statement

**Zhicheng Yang:** Writing – review & editing, Writing – original draft, Visualization, Validation, Software, Resources, Methodology, Investigation, Formal analysis, Data curation, Conceptualization. **Xiaobing Liu:** Writing – review & editing, Supervision, Resources, Data curation, Conceptualization. **Jiangfeng Wang:** Writing – review & editing, Supervision, Resources, Conceptualization. **Xuedong Yan:** Writing – review & editing, Resources, Conceptualization. **Rui Shen:** Writing – review & editing, Data curation, Conceptualization. **Zhengqi Huo:** Writing – review & editing, Conceptualization.

#### Declaration of competing interest

The authors declare that they have no known competing financial interests or personal relationships that could have appeared to influence the work reported in this paper.

#### Acknowledgments

This research was partially supported by a project funded by National Key Research and Development Program of China (No.2023YFC3009600), National Natural Science Foundation of China (No. 72242102), and Central Guiding Local Science and Technology Development Fund Projects of Hebei Province (No.236Z0802G).

#### References

- [1] He JH, et al. Measuring urban spatial interaction in Wuhan Urban Agglomeration, Central China: a spatially explicit approach. *Sustain Citi Soc* 2017;32:569–83.
- [2] Fang C, Yu D. Urban agglomeration: an evolving concept of an emerging phenomenon. *Landslides Urban Plan* 2017;162:126–36.
- [3] Heuermann DF, Schmieder JF. The effect of infrastructure on worker mobility: evidence from high-speed rail expansion in Germany. *J Econ Geogr* 2019;19(2): 335–72.
- [4] Wei G, et al. Influence mechanism of transportation integration on industrial agglomeration in urban agglomeration theory—taking the Yangtze River Delta Urban Agglomeration as an example. *Appl Sci* 2022;12(16).
- [5] Hu Y, Chen Y. Coupling of urban economic development and transportation system: an urban agglomeration case. *Sustainability* 2022;14(7).
- [6] Lyapin S, et al. Stages to create and develop module of regional intelligent transportation and logistics system. *Transport Res Proced* 2020;45:939–46.
- [7] Li Y, et al. Spatiotemporal influence of built environment on intercity commuting trips considering nonlinear effects. *J Transp Geogr* 2024;114.

- [8] Huang H-J, et al. Transportation issues in developing China's urban agglomerations. *Transp Policy* 2020;85:A1–22.
- [9] Mu X, Fang C, Yang Z. Spatio-temporal evolution and dynamic simulation of the urban resilience of Beijing-Tianjin-Hebei urban agglomeration. *J Geograph Sci* 2022;32(9):1766–90.
- [10] Liu X, et al. Network resilience. *Phys Rep* 2022;971:1–108.
- [11] Osei-Asamoah A, Lownes NE. Complex network method of evaluating resilience in surface transportation networks. *Transport Res Record: J Transport Res Board* 2014;2467(1):120–8.
- [12] Serdar MZ, Koç M, Al-Ghamdi SG. Urban transportation networks resilience: indicators, disturbances, and assessment methods. *Sustain Citi Soc* 2022;76.
- [13] Janić M. Modelling the resilience, friability and costs of an air transport network affected by a large-scale disruptive event. *Transport Res Part A: Policy Pract* 2015; 71:1–16.
- [14] Besinović N, Ferrari Nassar R, Szymula C. Resilience assessment of railway networks: combining infrastructure restoration and transport management. *Reliab Eng Syst Safe* 2022;224.
- [15] Gonçalves LAPJ, Ribeiro PJG. Resilience of urban transportation systems. Concept, characteristics, and methods. *J Transp Geogr* 2020;85.
- [16] Voltes-Dorta A, Rodríguez-Déniz H, Stau-Sánchez P. Vulnerability of the European air transport network to major airport closures from the perspective of passenger delays: ranking the most critical airports. *Transport Res Part A: Policy Pract* 2017; 96:119–45.
- [17] Ouyang M, et al. Comparisons of complex network based models and real train flow model to analyze Chinese railway vulnerability. *Reliab Eng Syst Safe* 2014; 123:38–46.
- [18] Yang Y, et al. Robustness assessment of urban rail transit based on complex network theory: a case study of the Beijing Subway. *Safe Sci* 2015;79:149–62.
- [19] Wang Y, et al. Vulnerability analysis of the Chinese coupled aviation and high-speed railway network. *Chin J Aeronaut* 2022;35(12):189–99.
- [20] Li T, Rong L, Yan K. Vulnerability analysis and critical area identification of public transport system: a case of high-speed rail and air transport coupling system in China. *Transport Res Part A: Policy Pract* 2019;127:55–70.
- [21] Hong L, et al. Time-varied accessibility and vulnerability analysis of integrated metro and high-speed rail systems. *Reliab Eng Syst Safe* 2020;193.
- [22] Ma F, et al. Exploring the robustness of public transportation for sustainable cities: a double-layered network perspective. *J Clean Product* 2020;265.
- [23] Li T, Rong L. Resilience of air Transport Network with the Complementary Effects of High-Speed Rail Network. In: 2019 IEEE 19th International Conference on Software Quality, Reliability and Security Companion (QRS-C); 2019. p. 348–53.
- [24] Chen M, Lu H. Analysis of Transportation Network Vulnerability and Resilience within an Urban Agglomeration: case Study of the Greater Bay Area, China. *Sustainability* 2020;12(18).
- [25] Li C, et al. Invulnerability simulation of urban agglomeration passenger transport network under incomplete information attack strategy. *Adv Civil Eng* 2021;2021: 1–12.
- [26] Bak P, Tang C, Wiesenfeld K. SELF-ORGANIZED CRITICALITY - AN EXPLANATION OF 1/F NOISE. *Phys Rev Lett* 1987;59(4):381–4.
- [27] Wu JJ, et al. Congestion in different topologies of traffic networks. *Europhys Lett* 2006;74(3):560–6.
- [28] Shen Y, et al. Model of node traffic recovery behavior and cascading congestion analysis in networks. *Physica a-Statist Mech Applic* 2020;545.
- [29] Duan J, Li D, Huang H-J. Reliability of the traffic network against cascading failures with individuals acting independently or collectively. *Transport Res Part C: Emerg Technolog* 2023;147.
- [30] Hao Y, et al. Improving resilience of high-speed train by optimizing repair strategies. *Reliab Eng Syst Safe* 2023;237.
- [31] Zhong J, et al. Network endurance against cascading overload failure. *Reliab Eng Syst Safe* 2020;201.
- [32] Wang N, Wu M, Yuen KF. A novel method to assess urban multimodal transportation system resilience considering passenger demand and infrastructure supply. *Reliab Eng Syst Safe* 2023;238.
- [33] Motter AE, Lai YC. Cascade-based attacks on complex networks. *Phys Rev E* 2002; 66(6).
- [34] Zhao Z, Zhang P, Yang H. Cascading failures in interconnected networks with dynamical redistribution of loads. *Physica A: Statist Mech Applic* 2015;433: 204–10.
- [35] Sendiña-Nadal I, et al. Study of robustness in functionally identical coupled networks against cascading failures. *Plos One* 2016;11(8).
- [36] Zhang Z-H, et al. A novel load capacity model with a tunable proportion of load redistribution against cascading failures. *Secur Commun Netw* 2018;2018:1–7.
- [37] Hao Y, Jia L, Wang Y. Robustness of weighted networks with the harmonic closeness against cascading failures. *Physica A: Statist Mech Applic* 2020;541.
- [38] Hao Y, et al. A multi-objective optimization model for identifying groups of critical elements in a high-speed train. *Reliab Eng Syst Safe* 2023;235.
- [39] Jin K, et al. Cascading failure in urban rail transit network considering demand variation and time delay. *Physica A: Statist Mech Applic* 2023;630.
- [40] Fn Y, Wang L, Chen MZQ. Robustness of controllability for scale-free networks based on a nonlinear load-capacity model. In: 14th IFAC Symposium on Large Scale Complex Systems - Theory and Applications (IFAC LSS); 2016.
- [41] Liu Z, et al. Evaluating the dynamic resilience of the multi-mode public transit network for sustainable transport. *J Clean Product* 2022;348.
- [42] Zhang D-m, et al. Resiliency assessment of urban rail transit networks: shanghai metro as an example. *Safe Sci* 2018;106:230–43.
- [43] Lee C-C, et al. Quantitative measures for integrating resilience into transportation planning practice: study in Texas. *Transport Res Part D: Transp Environ* 2022;113.
- [44] Zhou Y, Wang J, Yang H. Resilience of transportation systems: concepts and comprehensive review. *IEEE Transact Intell Transport Syst* 2019;20(12):4262–76.
- [45] Wang J, et al. Measurement of functional resilience of transport network: the case of the Beijing subway network. *Transp Policy* 2023;140:54–67.
- [46] Xu Z, Chopra SS. Network-based Assessment of Metro Infrastructure with a Spatial-temporal Resilience Cycle Framework. *Reliab Eng Syst Safe* 2022;223.
- [47] Gorji M-A, Akbarzadeh M, Shetab-Boushehri S-N. Evaluation and improvement of the urban transportation networks resilience in short-term non-recurring traffic congestion: a novel graph connectivity-based criteria. *Transport Eng* 2022;10.
- [48] Kamga CN, Mouskos KC, Paaswell RE. A methodology to estimate travel time using dynamic traffic assignment (DTA) under incident conditions. *Transport Res Part C: Emerg Technolog* 2011;19(6):1215–24.
- [49] Yin K, et al. An integrated resilience assessment model of urban transportation network: a case study of 40 cities in China. *Transport Res Part A: Policy Pract* 2023; 173.
- [50] Adjetey-Bahun K, et al. A model to quantify the resilience of mass railway transportation systems. *Reliab Eng Syst Safe* 2016;153:1–14.
- [51] Ganin AA, et al. Resilience and efficiency in transportation networks. *Sci Adv* 2017; 3(12):e1701079.
- [52] Nogal M, et al. Resilience of traffic networks: from perturbation to recovery via a dynamic restricted equilibrium model. *Reliab Eng Syst Safe* 2016;156:84–96.
- [53] Liao T-Y, Hu T-Y, Ko Y-N. A resilience optimization model for transportation networks under disasters. *Nat Hazard* 2018;93:469–89.
- [54] Calabrese F, et al. Understanding individual mobility patterns from urban sensing data: a mobile phone trace example. *Transport Res Part C: Emerg Technolog* 2013; 26:301–13.
- [55] Gonzalez MC, Hidalgo CA, Barabasi A-L. Understanding individual human mobility patterns. *Nature* 2008;453(7196):779–82.
- [56] Marada M, et al. Interurban mobility: eurhythmic relations among metropolitan cities monitored by mobile phone data. *Appl Geogr* 2023;156.
- [57] Zhang W, et al. Measuring megaregional structure in the Pearl River Delta by mobile phone signaling data: a complex network approach. *Cities* 2020;104.
- [58] Zhang B, et al. Delineating urban functional zones using mobile phone data: a case study of cross-boundary integration in Shenzhen-Dongguan-Huizhou area. *Comput Environ Urban Syst* 2022;98.
- [59] Li F, et al. Explore the recreational service of large urban parks and its influential factors in city clusters – Experiments from 11 cities in the Beijing-Tianjin-Hebei region. *J Clean Product* 2021;314.
- [60] Li T, Rong L. Spatiotemporally complementary effect of high-speed rail network on robustness of aviation network. *Transport Res Part A: Policy Pract* 2022;155: 95–114.
- [61] Jiao J, Zhang F, Liu J. A spatiotemporal analysis of the robustness of high-speed rail network in China. *Transport Res Part D: Transp Environ* 2020;89.
- [62] De Bona AA, et al. Analysis of public bus transportation of a Brazilian City based on the theory of complex networks using the P-space. *Math Probl Eng* 2016;2016: 1–12.
- [63] Zhang Y, Ng ST. Robustness of urban railway networks against the cascading failures induced by the fluctuation of passenger flow. *Reliab Eng Syst Safe* 2022; 219.
- [64] Cheng G, Wilmot CG, Baker EJ. A destination choice model for hurricane evacuation. In: proceedings of the 87th annual meeting transportation research board; 2008.
- [65] Zhang Z, et al. Evacuation based on spatio-temporal resilience with variable traffic demand. *J Manag Sci Eng* 2021;6(1):86–98.
- [66] Xu, Z., S.S.J.R.E. Chopra, and S. Safety, Network-based assessment of metro infrastructure with a spatial-temporal resilience cycle framework. 2022. 223: p. 108434.
- [67] Galaitis, S., et al., The need to reconcile concepts that characterize systems facing threats. 2021. 41(1): p. 3–15.
- [68] Ganin, A.A., et al., Operational resilience: concepts, design and analysis. 2016. 6 (1): p. 1–12.
- [69] Fang, C., et al., On the resilience assessment of complementary transportation networks under natural hazards. 2022. 109: p. 103331.
- [70] Pan, X., et al., Resilience model and recovery strategy of transportation network based on travel OD-grid analysis. 2022. 223: p. 108483.
- [71] Wang, J., et al., Measurement of functional resilience of transport network: the case of the Beijing subway network. 2023. 140: p. 54–67.
- [72] Chen, X., et al., Resilience measurement and analysis of intercity public transportation network. 2024. 131: p. 104202.
- [73] Sun X, et al. Multiple airport regions based on inter-airport temporal distances. *Transport Res Part E: Logist Transport Rev* 2017;101:84–98.
- [74] Clark, K.L., et al., Resilience of the US national airspace system airport network. 2018. 19(12): p. 3785–3794.
- [75] Yadav, N., S. Chatterjee, and A.R.J.S.R. Ganguly, Resilience of urban transport network-of-networks under intense flood hazards exacerbated by targeted attacks. 2020. 10(1): p. 10350.